



**HAL**  
open science

## Modified Direct Torque Control of PMSM Drives using Dither Signal Injection and Non-Hysteresis Controllers

M Kadjoudj, S Taibi, N Golea, Mohamed Benbouzid

► **To cite this version:**

M Kadjoudj, S Taibi, N Golea, Mohamed Benbouzid. Modified Direct Torque Control of PMSM Drives using Dither Signal Injection and Non-Hysteresis Controllers. *Electromotion*, 2006, 13 (4), pp.262-270. hal-01184270

**HAL Id: hal-01184270**

**<https://hal.science/hal-01184270>**

Submitted on 13 Aug 2015

**HAL** is a multi-disciplinary open access archive for the deposit and dissemination of scientific research documents, whether they are published or not. The documents may come from teaching and research institutions in France or abroad, or from public or private research centers.

L'archive ouverte pluridisciplinaire **HAL**, est destinée au dépôt et à la diffusion de documents scientifiques de niveau recherche, publiés ou non, émanant des établissements d'enseignement et de recherche français ou étrangers, des laboratoires publics ou privés.

# Modified Direct Torque Control of PMSM Drives using Dither Signal Injection and Non-Hysteresis Controllers

M. Kadjoudj, S.Taibi, N. Golea, M.E.H. Benbouzid

**Abstract** - The DTC of voltage source inverter fed PMSM is based on hysteresis controllers of torque and flux. It has several advantages, namely, elimination of the mandatory rotor position sensor, less computation time and fast torque response. In addition, the stator resistance is the only parameter, which should be known and no reference frame transformation is required. The implementation of DTC in PMSM drives is described and the switching tables specific for an interior PMSM are derived. The conventional eight voltage-vector switching table, which is namely used in the DTC of induction motor, does not seem to regulate the torque and stator flux in PMSM well when the motor operates at low speed. Modelling and simulation studies have both revealed that a six voltage-vector switching table is more appropriate for PMSM drive at low speed. Different switching algorithms using hysteresis and non-hysteresis controllers are proposed and the effectiveness of the strategies are analyzed and discussed. In addition, a modified method is proposed which introduces dither signal injection so that the flux and torque ripples are reduced.

**Index terms**—DTC, PMSM, Hysteresis and non-hysteresis controllers, switching tables.

## 1. Introduction.

In the existing literature, many algorithms have been suggested for the DTC control. The eight voltage-vector switching scheme seems to be suitable only for high speed operation of the motor while at low speed the six voltage-vector switching scheme, avoiding the two zero voltage-vectors, seems to be appropriate for the permanent magnet synchronous motor drive [1] [2].

The voltage vector strategy using switching table is widely researched and commercialized, because it is very simple in concept and very easy to be implemented. The stator fluxes linkage are calculated from voltage and current models PMSM drive. The DTC is increasingly drawing interest because of,

- Simplicity of its structure.
- Elimination of the current controllers.
- Inherent delays.
- Elimination of rotor position sensor.

The switching frequency can not practically increased when the hysteresus band width is sufficiently reduced because of delay time in estimating current and flux. In order to overcome this problem, a modified DTC method is proposed

introducing a dither signal by superposing a high frequency and small amplitude triangular or sine wave on the torque and flux errors as it is shown in figure 2. According to the modelling results, the stator flux and torque ripples were reduced to 25% compared to those of conventional scheme and this enables the controller to raise the switching frequency regardless of the delay time and also makes acoustically silent drive possible.

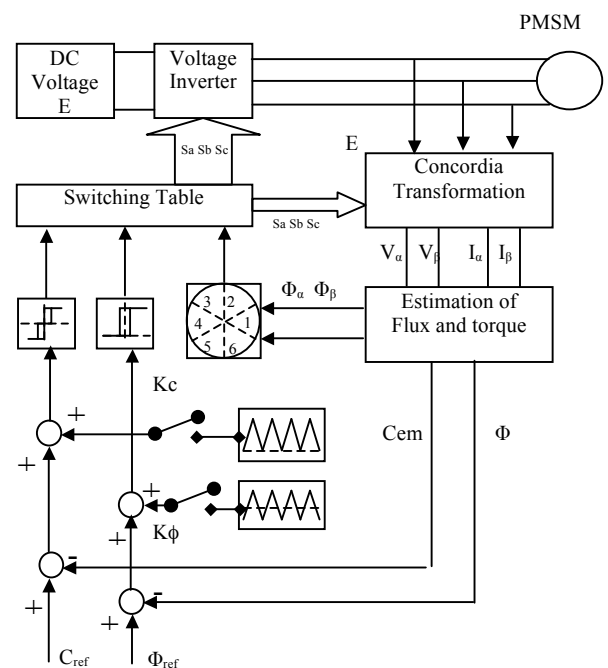


Fig. 1. Modified DTC control

Two direct torque control schemes for PMSM drive with injection of dither signal and with non hysteresis controllers are proposed in this paper, which features in low torque and flux ripples and almost fixed switching frequency. The torque and flux ripples have been significantly reduced if compared with those of the basic DTC.

## 2. Machine Equations

The motor considered in this paper is an interior PMSM which consists of a three phase stator windings and a PM rotor. The voltage equations in a synchronous reference frame can be derived as follows [3][4],

$$V_d = R_s \cdot I_d + \frac{d\phi_d}{dt} - \omega_r \cdot \phi_q \quad (1)$$

$$V_q = R_s \cdot I_q + \frac{d\phi_q}{dt} + \omega_r \cdot \phi_d \quad (2)$$

Where the direct and quadrature axis flux linkages are,

$$\phi_d = L_d \cdot I_d + \phi_f \quad (3)$$

$$\phi_q = L_q \cdot I_q \quad (4)$$

The electromagnetic torque of the motor can be evaluated as follows,

$$C = \frac{3}{2} n_p \cdot \{ \phi_f \cdot I_q + (L_d - L_q) \cdot I_d \cdot I_q \} \quad (5)$$

The motor dynamics can be simply described by the equation (6).

$$\frac{J}{n_p} \frac{d\omega_r}{dt} + \frac{f}{n_p} \cdot \omega_r = C_{em} - C_{st} \quad (6)$$

By using the concept of the field orientation, it can be assumed that the d-axis current is controlled to be zero. Thus, the PMSM has the best dynamic performance and also operates in the most efficient state. Under this assumption, the contribution of the second term of the electric torque equation becomes effectively negligible and the reduced dynamic model of the PMSM is given by the following equations.

$$\frac{dI_q}{dt} = \frac{1}{L_q} V_q - \frac{R_s}{L_q} I_q - \frac{\phi_f}{L_q} \omega_r \quad (7)$$

$$\frac{J}{n_p} \frac{d\omega_r}{dt} = K_T \cdot I_q - \frac{f}{n_p} \omega_r - C_{st} \quad (8)$$

$$\frac{d\theta}{dt} = \omega_r \quad (9)$$

## 3. DTC Algorithm

The electromagnetic torque equation can be expressed in terms of the stator flux linkage and its angle with respect to the rotor flux linkage as follows :

$$C = 0.75 \cdot n_p \left[ \frac{2 \cdot \phi_f \cdot \phi_s}{L_d} \cdot \sin(\delta) + \phi_s^2 \left\{ \frac{1}{L_q} - \frac{1}{L_d} \right\} \sin(2\delta) \right] \quad (10)$$

For a surface magnet motor, equation 10 becomes,

$$C = 1.5 \cdot n_p \cdot \frac{\phi_f \cdot \phi_s}{L} \cdot \sin(\delta) \quad (11)$$

The angle between the stator and rotor flux linkages, noted  $\delta$ , is the load angle when the stator resistance is neglected. In the steady state, the load angle is constant corresponding to a load torque. Both the stator and rotor fluxes rotate at the synchronous speed. In transient state, the load angle varies and the flux vectors rotate at different speeds. The relationship between torque  $C$  and  $\delta$  may be linear in some cases, and may not be linear in others cases as depicted by figure 2.

Figure 2 shows the torque-load angle characteristics of PMSM drive. When the flux amplitude is at  $0.5\phi_f$ ,  $0.75\phi_f$ ,  $\phi_f$ ,  $1.5\phi_f$ ,  $2\phi_f$  and  $3\phi_f$ . For the two last cases, the derivative of torque near zero crossing is negative. Then, the DTC can not be applied. The condition for positive derivative of the torque with respect to the load angle is given by equation (12). For obtaining fast dynamic torque response, the amplitude of stator flux linkage should be chosen according to relation (12).

$$\phi_s < \frac{L_q}{L_q - L_d} \cdot \phi_f \quad (12)$$

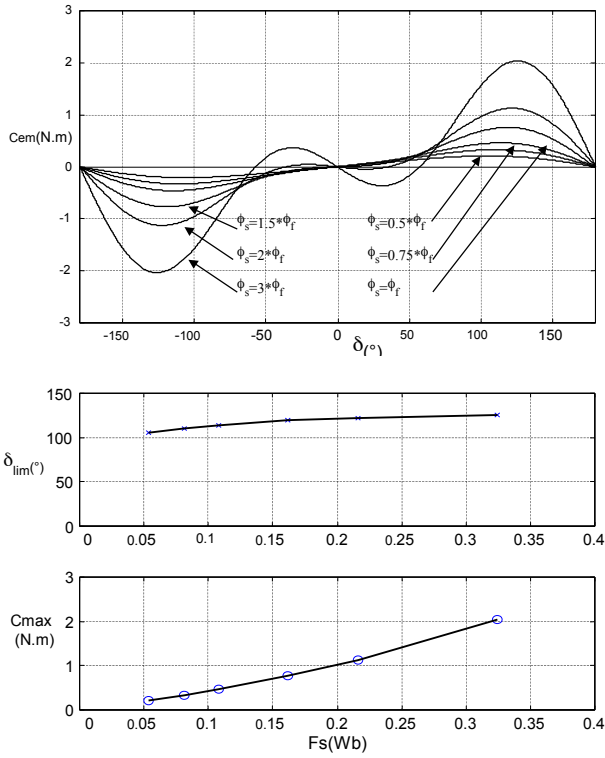


**Fig. 2.** Torque – angle characteristics of PMSM

The derivative of torque  $dC/dt$  in equation (10) is positive if  $-\pi/2 < \delta < \pi/2$ . Then, the increase of torque is proportional to the increase of the angular velocity  $\delta$ . In other words, the stator flux  $\phi_s$  should be controlled in such a way that the amplitude is kept constant and the rotating speed is controlled as fast possible to obtain the maximum change in actual torque. There are six non-zero voltage vectors  $V_1$ - $V_6$  and two zero voltage vectors  $V_7$ - $V_8$ .

- $V_1(1 -1 -1) \Rightarrow S_a=1 ; S_b=-1, S_c=-1.$
- $V_2(1 1 -1) \Rightarrow S_a=1 ; S_b=1, S_c=-1.$
- $V_3(-1 1 -1) \Rightarrow S_a=-1; S_b=1, S_c=-1.$
- $V_4(-1 1 1) \Rightarrow S_a=-1; S_b=1, S_c=1.$
- $V_5(-1 -1 1) \Rightarrow S_a=-1; S_b=-1, S_c=1.$
- $V_6(1 -1 1) \Rightarrow S_a=1 S_b=-1, S_c=1.$
- $V_7(-1 -1 -1) \Rightarrow S_a=-1; S_b=-1, S_c=-1.$
- $V_8(1 1 1) \Rightarrow S_a=1; S_b=1, S_c=1.$

The two zero voltage vectors are at the origin and the six non-zero voltage vectors are  $60^\circ$  apart from each other in voltage vector plane as depicted by figure 3.

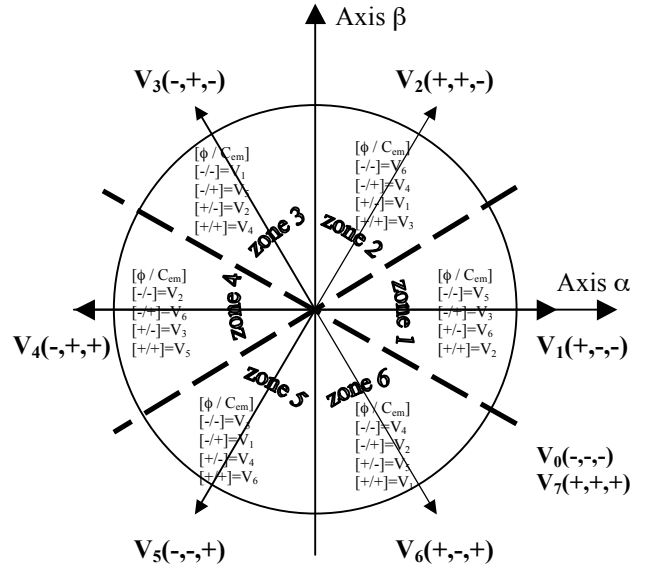


**Fig. 3.** Sectors and voltage vectors.

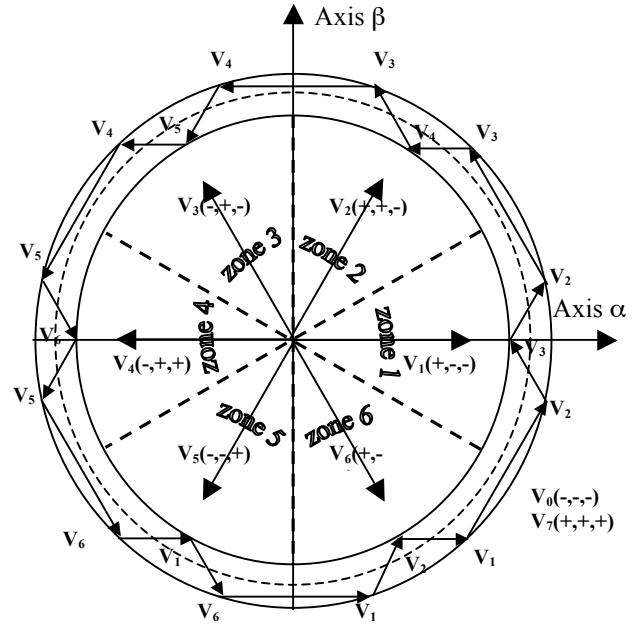


**Fig. 4.** Control of stator flux linkage with selected stator voltage vectors.

During the switching intervals, each applied voltage vector remains constant and the stator fluxes linkages are given in the stationary reference frame as

$$\phi_{\alpha}(k+1) = \phi_{\alpha}(k) + h[V_{\alpha}(k) - R_s I_{\alpha}(k)] \quad (13)$$

$$\phi_{\beta}(k+1) = \phi_{\beta}(k) + h[V_{\beta}(k) - R_s I_{\beta}(k)] \quad (14)$$

Neglecting the stator resistance, equations 13 and 14 implies that the tip of the stator vector will move in the direction of the applied voltage vector in a straight line as indicated in figure 4. For controlling the amplitude of the stator flux, the voltage vector plane is divided into six regions. Each of this region is  $60^\circ$  wide. In each region, two adjacent voltage vectors may be selected to increase or decrease the stator flux amplitude and give a minimum switching frequency.

The six-region control is distinguished based on the inequalities:

$$-\frac{\pi}{6} + (1-N) \cdot \frac{\pi}{3} \leq \theta(N) < \frac{\pi}{6} - (1-N) \cdot \frac{\pi}{3}$$

In figure 4, the space between the two circles represents the hysteresis band in stator flux linkage amplitude which in turn is equal to the rated flux when operation below the based speed is called for. For field weakening, these two circles contract inward.

Figure 5 shows the control structure for selecting the voltage vectors and keeping torque and flux linkage within pre-selected hysteresis bands.

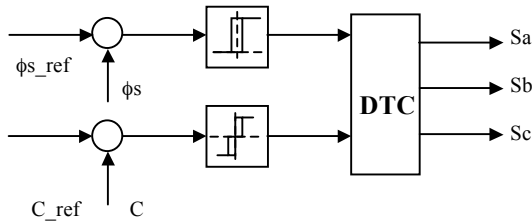


**Fig. 5.** Torque and flux hysteresis controllers.

#### 4. Voltage Switching Tables for DTC

The torque and flux hysteresis controllers select the appropriate voltage vectors. Tables 1 and 2 indicate the six and eight voltage vectors switching strategies, in each region  $C$  and  $\phi$  are increasing or decreasing functions of time. From table 2, it is clear that when the torque is increasing

or decreasing, the flux linkage can be increased or decreased by selecting alternatively one of the six non zero voltage vectors and one of the two zero voltage vectors.

**Table 1.** The six voltage vectors switching table

		Z=1	Z=2	Z=3	Z=4	Z=5	Z=6
$R_s=1$ ( $\phi \uparrow$ )	$R_c=1$ ( $C \uparrow$ )	$V_2$	$V_3$	$V_4$	$V_5$	$V_6$	$V_1$
	$R_c=0$ ( $C \downarrow$ )	$V_6$	$V_1$	$V_2$	$V_3$	$V_4$	$V_5$
$R_s=0$ ( $\phi \downarrow$ )	$R_c=1$ ( $C \uparrow$ )	$V_3$	$V_4$	$V_5$	$V_6$	$V_1$	$V_2$
	$R_c=0$ ( $C \downarrow$ )	$V_5$	$V_6$	$V_1$	$V_2$	$V_3$	$V_4$

From table 1, the torque and flux are increased or decreased by selecting only the six non zero voltage vectors. The torque is changed by reversing the movement of the stator flux vector at each state of the hysteresis controller output.

**Table 2.** The eight classic voltage vectors switching table

		Z=1	Z=2	Z=3	Z=4	Z=5	Z=6
$R_s=1$ ( $\phi \uparrow$ )	$R_c=1$ ( $C \uparrow$ )	$V_2$	$V_3$	$V_4$	$V_5$	$V_6$	$V_1$
	$R_c=0$ ( $C \downarrow$ )	$V_7$	$V_0$	$V_7$	$V_0$	$V_7$	$V_0$
$R_s=0$ ( $\phi \downarrow$ )	$R_c=1$ ( $C \uparrow$ )	$V_3$	$V_4$	$V_5$	$V_6$	$V_1$	$V_2$
	$R_c=0$ ( $C \downarrow$ )	$V_0$	$V_7$	$V_0$	$V_7$	$V_0$	$V_7$

The use of the six voltage vectors switching table implies that the stator flux linkage is always kept in motion, making it to go forward and backward in order to regulate the torque loop. For controlling the amplitude of stator flux and therefore for changing the torque, zero voltage vectors  $V_7$  and  $V_0$  are not used in PMSM drives.

In tables 1 and 2,  $R_s$  and  $R_c$  are the outputs of the hysteresis controllers.  $Z=1, \dots, 6$  represent the regions numbers for the stator flux linkage positions.

To study the performance of the DTC control, the simulation of the system was conducted using Matlab programming environment. Figure 6 shows that the motor can follow the command torque

very well. However, relatively high torque ripples are observed. The estimated stator flux has the same form of the flux reference and figure 6 shows how the voltage vectors are selected for keeping  $\phi_s$  within hysteresis band when  $\phi_s$  is rotating in the counter clockwise direction.

Table 3. Switching table with three levels controller.

		Z=1	Z=2	Z=3	Z=4	Z=5	Z=6
$R_s=1$ ( $\phi \uparrow$ )	$R_c=1$ ( $C \uparrow$ )	V <sub>2</sub>	V <sub>3</sub>	V <sub>4</sub>	V <sub>5</sub>	V <sub>6</sub>	V <sub>1</sub>
	$R_c=0$	V <sub>7</sub>	V <sub>0</sub>	V <sub>7</sub>	V <sub>0</sub>	V <sub>7</sub>	V <sub>0</sub>
	$R_c=-1$ ( $C \downarrow$ )	V <sub>6</sub>	V <sub>1</sub>	V <sub>2</sub>	V <sub>3</sub>	V <sub>4</sub>	V <sub>5</sub>
$R_s=0$ ( $\phi \downarrow$ )	$R_c=1$ ( $C \uparrow$ )	V <sub>3</sub>	V <sub>4</sub>	V <sub>5</sub>	V <sub>6</sub>	V <sub>1</sub>	V <sub>2</sub>
	$R_c=0$	V <sub>0</sub>	V <sub>7</sub>	V <sub>0</sub>	V <sub>7</sub>	V <sub>0</sub>	V <sub>7</sub>
	$R_c=-1$ ( $C \downarrow$ )	V <sub>5</sub>	V <sub>6</sub>	V <sub>1</sub>	V <sub>2</sub>	V <sub>3</sub>	V <sub>4</sub>

The PMSM was simulated under the DTC drive system at high and low speed. Figure 7 revealed loss of control over torque and stator flux when the zero voltage algorithm is used, these could not be attributed to factors such offsets in the measurements of motor terminal quantities and the variation of stator resistance which are known sources of problems in DTC. It is seen however that the ripples in torque and flux characteristics are considerably lower when the eight voltage vectors in table 2 are used. This implies that table 2 is more appropriate for high speed operations.

As mentioned from equation (10), the torque is proportional to the angle  $\delta$ , which must be changed quickly. Unlike the asynchronous motor where change of slip frequency brought about by applying zero voltage vectors, the angle  $\delta$  in the case of PMSM is determined also by the position of the rotor flux linkage which is non zero at all times. To control torque at low speed, quick change of  $\delta$  can be obtained by avoiding the zero voltage vectors and by applying vectors which move the stator flux relative to rotor flux as quickly as possible. At high speed, this may not be necessary where the rotor move sufficiently to produce the required change in torque. The

conventional eight voltage vector switching table is normally used in the DTC of induction motors and does not seem to regulate the torque and stator flux in PMSM drive well when the motor operates at low speed.

To overcome the previously mentioned difficulties, an algorithm is proposed in table 3, which consists in combination of advantages of the two classic tables simultaneously and has advantage of conceptual simplicity. Modelling results for similar operating conditions with three levels torque hysteresis controller are presented in figure 9.

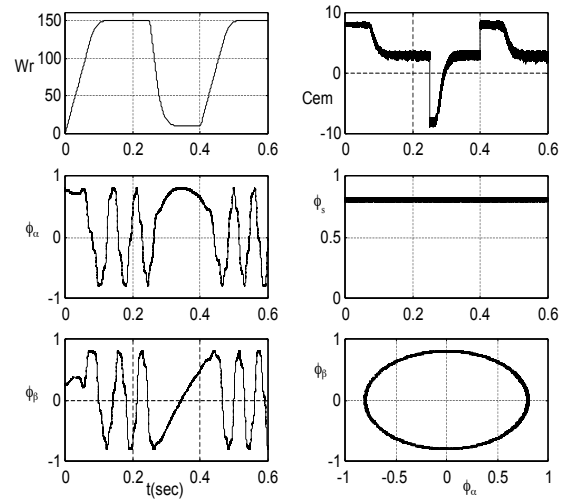


Fig. 6. DTC without zero voltage vectors.

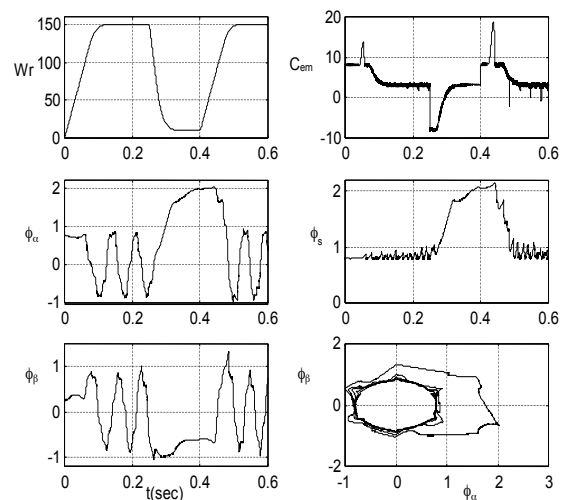
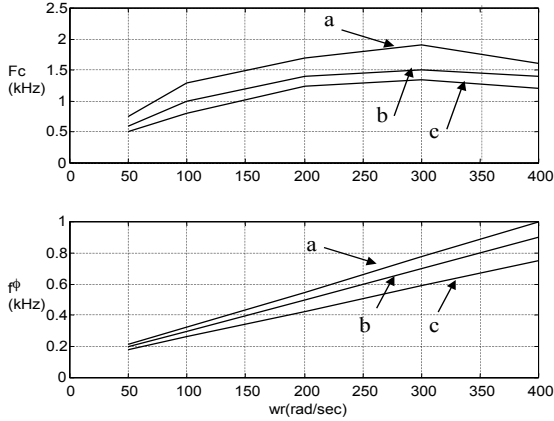


Fig. 7. DTC with zero voltage vectors

The hysteresis band has to be set large enough to limit the inverter switching frequency below a

certain level. The amplitude of the hysteresis band strongly influences the inverter performance such as torque and flux ripples, current harmonics and switching frequency.



**Fig 8.** Switching frequencies of torque and flux versus speed.  
a)  $\Delta C = \Delta\phi = 0.01$  b)  $\Delta C = \Delta\phi = 0.025$  c)  $\Delta C = \Delta\phi = 0.1$

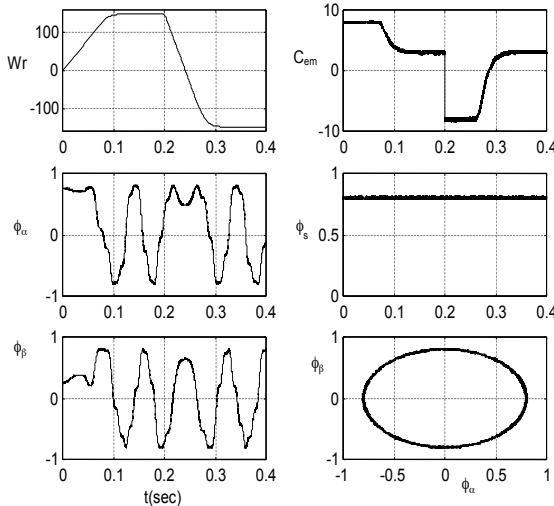


**Fig. 9.** DTC with three levels torque controller.

The switching frequency variation characteristic of the flux hysteresis controller is different from that of torque hysteresis controller. As shown in figure 8, the switching frequency has a maximum value in a medium speed range. For the flux controller, the switching frequency is proportional to the motor speed. This phenomenon makes flux and torque hysteresis controllers to have different contributions to the total switching frequency. It means that the amplitude of flux and torque hysteresis controllers should be regulated separately for effective utilisation of given total switching frequency controller command.

## 5. DTC with non-hysteresis controllers

Different switching algorithms using non-hysteresis controllers are proposed. The difference between the actual stator flux and its reference value and the difference between the motor torque and its reference value are controlled over a hysteresis cycle with defined levels which dictate the inverter switching pattern.

In this technique, there is no hysteresis controller and history of the flux and torque errors do not play any role in the switching of the inverter. This non-hysteresis controller technique can be classified based on the number of the error levels. Advantages of the later technique are,

- Simplicity of the flux and torque controllers compared with the hysteresis controllers.
- Lower switching frequency.
- Limitation of the amplitude of the current harmonics.

### 5.1. Multi bands torque and flux controllers

The control algorithm of this first technique can be summarized as follows,

Rule A $e_c > \Delta C$	then	$R_c = 0$
$0 \leq e_c \leq \Delta C$	then	$R_c = 1$
$-\Delta C_1 \leq e_c < 0$	then	$R_c = 2$
$-\Delta C_2 \leq e_c < -\Delta C_1$	then	$R_c = 3$
$e_c < -\Delta C_2$	then	$R_c = 4$

Rule B $e_\phi > \Delta\phi$	then	$R_\phi = 0$
$0 \leq e_\phi \leq \Delta\phi$	then	$R_\phi = 1$
$-\Delta\phi \leq e_\phi < 0$	then	$R_\phi = 2$
$e_\phi < -\Delta\phi$	then	$R_\phi = 3$

The predefined error level of the torque controller is divided into two parts and the table 4 gives the switching sequences.

Table 4. Switching sequences of the control.

		$R_C$						
		0	1	2	3	4		
		$N$						
$R_s$	0	Z+1	Z	Z	0	Z-1		
	1	Z+1	Z+1	0	0	Z-1		
	2	Z+2	Z+2	0	0	Z-2		
	3	Z+2	Z+3	Z+3	0	Z-2		
$N$	0	1	2	3	4	5	6	7
$S$	$V_0$	$V_1$	$V_2$	$V_3$	$V_4$	$V_5$	$V_6$	$V_7$

## 5.2. Dual band and triple band controllers

The control algorithm, with dual band flux controller and triple band torque controller, is summarized as follows,

Rule A:  $e_c > \Delta C$  then  $R_c = 1$   
 $-\Delta C \leq e_c \leq \Delta C$  then  $R_c = 0$   
 $e_c < -\Delta C$  then  $R_c = -1$

Rule B  $e_s > \Delta \phi$  then  $R_s = 1$   
 $e_s < -\Delta \phi$  then  $R_s = 0$

The flux is passive over the range  $[-\Delta \phi, \Delta \phi]$  in order to reduce the switching frequency and the programming effort. The inverter switching algorithm is identical to the classical DTC control.

## 5.3. Single band and triple band controllers

The inverter switching control is the same with the classical DTC technique. The difference with the last controller is that the decision range for flux controller is  $-\Delta \phi$  instead of  $[-\Delta \phi, \Delta \phi]$ .

Rule A:  $e_c > \Delta C$  then  $R_c = 1$   
 $-\Delta C \leq e_c \leq \Delta C$  then  $R_c = 0$   
 $e_c < -\Delta C$  then  $R_c = -1$

Rule B:  $e_s > -\Delta \phi$  then  $R_s = 1$   
 $e_s < -\Delta \phi$  then  $R_s = 0$

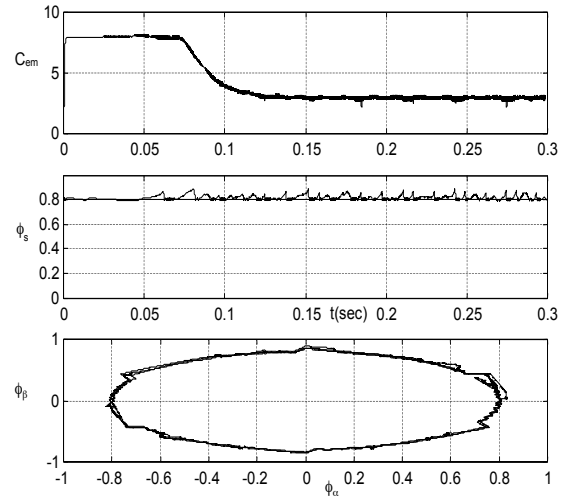


Fig. 10. Performance of the non-hysteresis controller.

The flux controller tries to keep the lower boundary of the flux. It is noted that the increase of the flux, with prevent acceleration of the motor, thus the upper boundary  $+\Delta \phi$  will be adjusted by the motor itself. This technique can be classified based on the number of the error levels and has advantages of,

- Lower switching frequency.
- Less memory required comparatively with the previous techniques.
- Reduced programming efforts.

## .6. Modified Control with Injection of Dither Signal

A modified DTC method introduces a dither signal by superposing a high frequency and small amplitude triangular or sine wave on the torque and flux errors. According to the several simulation results illustrated in figure 11, the stator flux and torque ripples were reduced compared to those of conventional scheme and this enables the controller to raise the switching frequency regardless of the delay time and also makes acoustically silent drive possible.



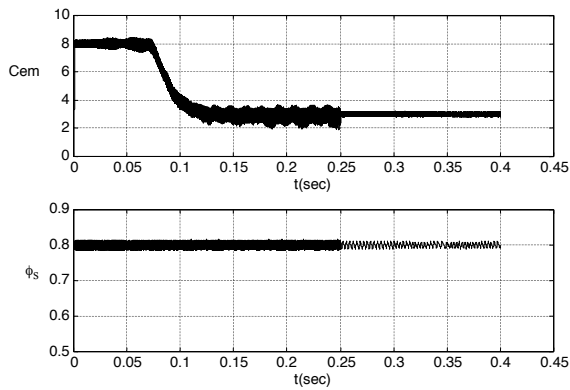


Fig. 11. Performance of the proposed DTC scheme.

## 7. Conclusion

The paper has presented a DTC control with combination of both the six and eight voltage vectors tables, which does not require a mechanical position. By controlling the stator flux linkage vector properly, the required torque can be produced with a fast response time.

The use of switching table with zero voltage vectors revealed loss of control, which could not attributed to factors such offsets in measurement and variation of stator resistance which are known sources of problems for the DTC.

The eight voltage vectors switching table is found to be preferable for high speed operating conditions with lower torque and stator flux ripples. The main advantages of the combined structure are,

- Stable and efficient structure.
- Improvement of torque ripple characteristic in a large speed range.
- Fast response and robustness merits entirely preserved.

The results indicate that the non-hysteresis controllers are cheaper and consume less electric power than the hysteresis controllers. The non-hysteresis controllers and modified DTC with dither signal have some important advantages as compared to the basic DTC algorithm such as, low switching frequency with identical sampling frequencies. Also, the logic of the modified

controller is simpler and more suitable for on-line applications. Consequently, the reduced switching pattern leads to a lower primary and operational costs of the inverter.

## APPENDIX RATED DATA OF THE SIMULATED PMSM

### Rated values

Frequency	50 Hz
Voltage ( $\Delta/Y$ )	220 V
Speed	1500 rpm
Torque	3 N.m
Pole pair ( $n_p$ )	2

### Rated parameters

$\phi_f$	0.314	Wb
$L_d$	0.0349	H
$L_q$	0.0627	H
$J$	0.003	kg.m <sup>2</sup>
$f$	0.00008	N.m.s
$R_s$	1.4	$\Omega$

## List of symbols

dq	Rotor direct and quadrature axis index
$\alpha\beta$	Components of the space phasor in $\alpha\beta$ coordinates
V	Voltage
I	Current
$\Phi_f$	Permanent magnet flux
$\Phi_s$	Stator flux linkage
$\theta_s$	Position of the stator flux vector
$C_{em}$	Electromagnetic torque
$C_{st}$	Load torque
$\omega_r$	Rotor speed
$\theta$	Rotor position
p	Operator d/dt
J	Moment of inertia
F	Viscosity coefficient
R	Resistance
L	Inductance
$n_p$	Number of pole pairs
$R_\Phi, R_c$	Hysteresis controllers outputs
$f_\Phi, f_c$	Torque and flux switching frequencies
$\Delta C, \Delta\Phi$	Torque and flux hysteresis band

## References

- [1] T.M. Jahns, "motion control with PM machines," *Proc. of the IEEE*, vol. 82, n°8, pp.1241-1252; 1994..
- [2] L. Zhong, M.F.Rahman, W.Y.Hu, "Analysis of direct torque control in PMSM drives," *IEEE Trans. Power Electronics*, vol. 12, n°3, pp. 528-536, 1997.
- [3] M.N. Uddin and al., "Performance of current controllers for IPMSM drive," in *Proc. of the IEEE IAS Annual Meeting*, vol. 2, pp. 1018-1025, 1999.
- [4] M. Kadjoudj, R.Abdesmed, M.E. Benbouzid, C. Ghennai, "Current control of PMSM fed by two and three levels VSI," in *Proc. of EPE/PEMC*, Tuke (Slovakia), vol. 7, pp. 69-74, 2000.
- [5] J.K.Kang, S.K.Sul, "New direct torque control of induction motor for minimum torque ripple and constant switching frequency," *IEEE Trans. On ind. Appl.*, vol. 35, n°5, pp. 1076-1082, 1999.
- [6] S.K. Chung and al., "A new instantaneous torque control of PMSM for high performance direct drive applications," *IEEE Trans. Power Electronics*, vol. 13, n°3, pp. 388-400, 1998.
- [7] K.M. Rahman, "Variable Band hysteresis current controllers for PWM VSI," *IEEE Trans. Power Electronics*, vol. 12, n°6, pp. 964-970, 1997.
- [8] C. French, P. Acarnley, "Direct torque control of permanent magnet drives," *IEEE Trans. On ind. Appl.*, vol. 32, n°5, pp. 1080-1088. 1996.
- [9] C. Lascu, I. Boldea, F. Blabjerg, "A modified Direct torque control for induction motor sensorless drive," *IEEE Trans. On ind. Appl.*, vol. 36, n°1, pp. 22-30, 2000.
- [10] J.K.Kang, D. Chang, S.K.Sul, "DTC of induction machine with variable amplitude control of flux and torque hysteresis bands," *conf. of the IEEE*, vol. 1, pp. 640-642, 1999.
- [11] M. Kadjoudj, M.E. Benbouzid, C. Ghennai, D.Diallo, "A Robust hybrid current control for PMSM drives," *IEEE trans. on energy conversion*, vol. 19 No 1. pp. 109-115, 2004.
- [12] M. Kadjoudj, "Contribution to the control of the PMSM drives," PhD thesis, Batna university, October 2003.
- [13] J.Faiz, H.M.ZonooziM, "A Novel technique and control of stator flux of a salient pole PMSM in DTC method based on MTPF," *IEEE trans. on industrial electronics*, vol. 50 No 2. pp. 262-271, April 2003.
- [14] J.Luukko, O.Pyrhonen, M.Niemela, J.Pyrhonen "Limitation of the load angle in a direct torque controlled synchronous machine drive," *IEEE trans. on industrial electronics*, vol. 51 No 4. pp. 793-798, August 2004.
- [15] A.Llor, B.Allard, X.Lin-Shi, J.M.Rtif, "Comparison of DTC implementations for synchronous machines," 35<sup>th</sup> annual IEEE power electronics conference, Aachen Germany, pp. 3581-3587, 2004.
- [16] L.Tang, L.Zhong, M.Rahman and Y.Hu, "A Novel direct synchronous machine drive with fixed switching frequency," *IEEE trans. on power electronics*, vol. 19 No 2. pp. 262-271, Marsh 2004.
- [17] M.F.Rahman, M.E.Haque, L.Tang, L.Zhong, "Problems associated with the DTC of an interior PMSM drive and their remedies," *IEEE trans. on industrial electronics*, vol. 51 No 4. pp. 799-808, August 2004.
- [18] M.Pacas, J.Weber, "Predictive direct torque control for the PM synchronous machine," *IEEE trans. on industrial electronics*, vol. 52 No 5. pp. 1350-1356, October 2005.

Dr. Mohamed Kadjoudj

Dr. Soufiane Taibi

Prof. Noureddine Golea

*Department of Electrical Engineering*

*University of Batna*

*Chahid Med Boukhrouf*

*Batna 05000, Algeria*

*Email : Kadjoudj\_m@yahoo.fr*

Prof. Mohamed El Hachemi Benbouzid

*University of Brest, EA 4325 LBMS, Brest, France*

*Email: Mohamed.Benbouzid@univ-brest.fr*